

Spindle Assembly in the Absence of a RanGTP Gradient Requires Localized CPC Activity

*Thomas J. Maresca^{1,3}, *Aaron C. Groen^{2,3}, Jesse C. Gatlin^{1,3}, Ryoma Ohi⁴, Timothy J. Mitchison^{2,3}, Edward D. Salmon^{1,3}

¹Department of Biology
University of North Carolina at Chapel Hill
Chapel Hill, North Carolina 27599
USA

²Systems Biology Department
Harvard Medical School
Boston, MA 02445
USA

³Cell Division Group
Marine Biological Laboratory
Woods Hole, MA 02543
USA

⁴Department of Cell and Developmental Biology
Vanderbilt University Medical Center
Nashville, TN 37232
USA

*These authors contributed equally to this work

Correspondence:
Thomas J. Maresca
Phone: (919) 962-2354
Fax: (919) 962-1625
Email: tmaresca@gmail.com

Running Head: RanGTP Gradient-Independent Spindle Assembly

Summary

During animal cell division, a gradient of GTP-bound Ran is generated around mitotic chromatin [1, 2]. It is generally accepted that this RanGTP gradient is essential for organizing the spindle since it locally activates critical spindle assembly factors [3-5]. Here, we show in *Xenopus* egg extract, where the gradient is best characterized, that spindles can assemble in the absence of a RanGTP gradient. Gradient-free spindle assembly occurred around sperm nuclei but not around chromatin-coated beads and required the chromosomal passenger complex (CPC). Artificial enrichment of CPC activity within hybrid bead arrays containing both immobilized chromatin and the CPC supported local microtubule assembly even in the absence of a RanGTP gradient. We conclude that RanGTP and the CPC constitute the two major molecular signals that spatially promote microtubule polymerization around chromatin. Furthermore, we hypothesize that the two signals mainly originate from discrete physical sites on the chromosomes to localize microtubule assembly around chromatin: a RanGTP signal from any chromatin, and a CPC-dependent signal predominantly generated from centromeric chromatin.

Results and Discussion

Centrosomes, kinetochores, and chromatin each provide distinct microtubule-organizing sites or signals that contribute to mitotic spindle assembly [6-8]. Of these, only the chromatin-mediated signal is sufficient for spindle formation [9]. This signal is thought to consist of at least two molecular activities, a RanGTP signal generated by the chromatin-bound Ran-GEF RCC1, and an Aurora B signal generated by localization of Aurora B kinase as part of the chromosomal passenger complex (CPC). The function of the RanGTP signal is best understood; relatively high concentrations of RanGTP near chromatin DNA locally release spindle assembly factors (SAFs) from sequestration by importins [3-5]. Current models hypothesize that a RanGTP gradient provides an essential spatial cue for biasing microtubule polymerization to the vicinity of chromatin. While the CPC has been shown to contribute to anastral spindle assembly [10, 11], the molecular function of chromatin-bound CPC in this process is less well characterized than the RanGTP system. It is hypothesized that Aurora B stimulates microtubule assembly around chromosomes by locally inhibiting factors that promote microtubule catastrophes [11, 12].

The role of specific chromatin domains for signaling microtubule assembly is poorly understood. Specifically, the relative contribution, at a molecular level, of bulk chromatin versus centromeric chromatin to locally support microtubule polymerization is unclear. RCC1 localizes throughout chromatin [13] while the CPC, which also localizes along chromosome arms, is concentrated at the inner centromere [14]. Kinetochores have been shown to locally promote microtubule

nucleation and stabilization, and appear to play a key role in spindle assembly in some systems [15, 16].

Kinetics of Tubulin Polymerization During Spindle Assembly Around DNA-coated Beads and Sperm Nuclei

To quantify the role of centrosomes and kinetochores in spindle assembly dynamics, we performed time-lapse microscopy of spindles assembling around either chromatin-coated beads or sperm nuclei in *Xenopus* egg extracts. (Figure 1A; and Supplemental Data, Movies 1-3). Chromatin bead spindles lack centrosomes and kinetochores, while sperm nuclei that have replicated their DNA contain kinetochores and centrosomes. In sperm spindles, the centrosomal array rapidly disassembled concomitant with nuclear envelope breakdown (NEBD) and often dissociated from assembling structures (Supplemental Data, Movie 3), suggesting that centrosomes are not required for normal sperm spindle assembly.

Although detailed assembly kinetics differed from spindle to spindle, certain generalities emerged, shown in the representative curves (Figure 1B, C). A pronounced lag phase was observed before the detectable onset of microtubule polymerization around both chromatin beads and sperm nuclei. Once assembly started, the rate of increase in microtubule density, and the time taken to reach a plateau, was faster for sperm nuclei, independent of the presence of obvious centrosomes. We do not believe that this discrepancy is due to significant differences between the chromatin content of sperm versus

beads since the protocol used in this study yields beads with ~0.3 pg of DNA/bead [9] or $1/10^{\text{th}}$ the amount of DNA as a single sperm nucleus. Since every bead cluster imaged consisted of at least 10 beads there may actually be higher amounts of DNA present in the bead spindle reactions. Thus, we conclude that sperm nuclei contain molecular activities that accelerate microtubule polymerization relative to chromatin beads. While we cannot rule out centrosomes as contributing to the faster kinetics, the fact that nuclei without associated centrosomes accumulated polymer faster than bead clusters makes us favor the interpretation that chromatin-associated activities on the sperm are largely responsible for the faster kinetics.

Sperm Spindles, but not Bead Spindles, Assemble in the Absence of a RanGTP Gradient

RanGTP is required for spindle assembly around both sperm nuclei and DNA beads in egg extracts [4], but it is not clear if its activity must be spatially regulated to localize spindle assembly. To test this, we experimentally flattened the RanGTP gradient for each type of assembly reaction while providing a constant background concentration of RanGTP by adding two different Ran mutants to spindle assembly reactions. RanT24N mimics the nucleotide-free state of Ran and binds with high affinity to RCC1, inhibiting local production of RanGTP by chromatin [17, 18]. RanQ69L, a hydrolysis defective mutant, is constitutively GTP-bound [18]. On its own, Q69L promotes formation of asters throughout the extract, independent of chromatin [19-21]. We added excess

T24N to completely inhibit assembly (30 μ M). ~80% of sperm nuclei either had no associated microtubules or asters while >90% of bead clumps had no associated microtubules at this concentration (Figures 2A, B and not shown). We then titrated Q69L and looked for rescue of assembly (Q/T Reaction). When Q69L was added at ~15 μ M, we observed rescue of spindle assembly around ~80 % of sperm nuclei. (Figures 2A, B and Supplemental Data, Figure S1). Under these same conditions, chromatin beads failed to assemble microtubule structures (Figure 2A). Increasing the concentration of Q69L did not rescue assembly around beads and at higher levels promoted assembly of microtubule asters (not shown). By imaging with two different FRET reporters [2], we found that the mixture of T24N and Q69L completely flattened the spatial gradients of RanGTP and liberated SAFs around chromatin, replacing them with a uniform concentration of each that was higher than in normal extracts (Figure 2C and Supplemental Data, Figure S2). Thus, sperm nuclei can assemble bipolar spindles in the absence of a localized gradient of RanGTP, while chromatin beads cannot, suggesting that sperm nuclei provide additional spatial signals that promote microtubule polymerization.

The molecular function of Ran-regulated SAFs in directing microtubule polymerization around chromatin remains poorly characterized. Interestingly, SAF activation by Q69L in T24N-treated reactions could be bypassed by the addition of three-fold excess End-binding 1 (EB1), a treatment that globally promotes microtubule assembly in the extract (Figures 2D, E). Identical to the Q/T reactions, this treatment failed to rescue bead spindle assembly (Figure 2D).

EB1 promotes microtubule polymerization in *Xenopus* extract by increasing the rescue frequency and decreasing the catastrophe frequency of microtubules independent of RanGTP [22]. Thus, under conditions of enhanced microtubule polymerization, spindle assembly not only occurs without a RanGTP gradient, but also without the activation of SAFs by RanGTP. Since EB1 is not known to nucleate microtubules but rather promotes microtubule elongation, this data suggests that SAF activities need not directly nucleate microtubules to achieve spindle assembly around sperm nuclei. Further, this provides additional evidence that sperm chromatin contains other RanGTP-independent signals to specifically localize bipolar spindle assembly.

RanGTP Gradient-Independent Spindle Assembly Requires the CPC

A second spatial signal from chromatin is proposed to come from the chromosomal passenger complex (CPC), consisting of Aurora B, INCENP, Survivin and Borealin/DasraA [11, 23, 24]. We depleted INCENP, and observed spindle assembly defects in both sperm and bead reactions. In both cases bipolar spindles were much smaller, and nuclei and bead clusters lacking microtubules were observed (Figures 3A-C). The two types of reaction were similarly perturbed, showing that normal spindle assembly in both reactions depends on CPC activity. Interestingly, Q/T reactions no longer supported localized microtubule polymerization around sperm nuclei following immunodepletion of INCENP (Figures 3A, B). Small molecule inhibition of Aurora

B with VX-680 had the same effect as INCENP depletion in all experiments (not shown).

INCENP depletion effects do not distinguish if the CPC acts locally, near chromatin, or globally, to promote microtubule assembly. To observe possible local effects, we inhibited the catastrophe-promoting kinesin-13 MCAK using a function perturbing antibody that has the effect of stabilizing microtubules. Aurora B is thought to stimulate local microtubule assembly in part by inhibiting this kinesin [11]. MCAK inhibition greatly increased the size of the microtubule assemblies around sperm nuclei in INCENP deleted extracts (Figure 3D). As previously noted [11], this double inhibited reaction retains spatial control, as assembly occurs near chromatin. However, spatial control was lost when the mixture of T24N and Q69L was added to MCAK inhibited reactions (Figure 3D), suggesting that the RanGTP gradient provides a major microtubule localizing cue when INCENP is missing. When both the RanGTP/SAF and Aurora B/MCAK systems were made spatially uniform, microtubule assembly became completely delocalized from chromatin. These results are in agreement with previous findings that suggest that the RanGTP and CPC pathways function independently [11, 24].

Enrichment of CPC is Necessary and Sufficient for DNA Beads to Support RanGTP Gradient-Independent Spindle Assembly

The RanGTP gradient is essential for DNA beads to promote localized microtubule polymerization but it is not essential for sperm nuclei to do so. Since

INCENP is required for sperm nuclei to support RanGTP gradient-independent spindle assembly, we next examined whether artificial localization of the CPC could confer gradient-free spindle assembly activity to DNA beads. CPC-localizing beads were made by coating them with α -INCENP IgG. These were mixed with chromatin coated beads, and the mixed clusters were tested for their ability to promote spindle assembly in untreated extract. Both anti-INCENP and control IgG mixed clusters supported spindle assembly (Figure 4A). In extracts supplemented with T24N and Q69L, control hybrids failed to support spindle assembly, while anti-INCENP hybrids supported assembly of $\sim 4X$ as many bead-associated microtubule arrays and $>10X$ the number of bipolar spindles compared to controls (Figures 4B, C). Anti-INCENP beads alone supported assembly of microtubule arrays in Q/T-treated extract but failed to assemble bipolar structures (not shown).

The difference between beads and sperm cannot be attributed to differences between CPC levels on each chromatin source because sperm and beads had comparable levels of associated Aurora B and INCENP (Figure 4D). Thus, the centromere may provide a local environment that promotes Aurora B activity at a molecular level by localizing additional Aurora B activators and/or at a structural level by spatially organizing the CPC in a conformation that most efficiently activates Aurora B. The hybrid beads had significantly higher levels of Aurora B and INCENP and Aurora B appeared to be hyper-phosphorylated since multiple higher molecular-weight Aurora B bands were detectable by western blot (Figure 4D). This data shows that the sperm-mediated regulation of CPC, which

is lacking on DNA beads can be artificially provided by anti-INCENP coated beads. The ability of hybrids to support spindle assembly may be due to the significant enrichment of CPC and/or hyper-activation of Aurora B although the latter is most likely a consequence of the former. We conclude that locally concentrated CPC activity is able to spatially promote spindle assembly even when RanGTP levels are made uniform.

Two Microtubule Polymerization Signals Originating from Distinct Physical Sites on the Chromosome Contribute to Spindle Assembly

Our results provide significant insight into how microtubules are preferentially assembled around chromosomes during cell division. Release of SAFs by RanGTP most likely activates a gradient of microtubule stabilization. However, we have found that spatial localization of RanGTP per se is not absolutely required since localization of CPC is sufficient to target assembly to the vicinity of chromatin. Conversely, centromere-enriched CPC activity is not required for spindle assembly in egg extracts as spindles form around generic chromatin beads without centromeric DNA. Since clustering of INCENP has been shown to promote autoactivation of Aurora B [24], centromeric clustering of CPC likely provides a threshold of Aurora B activity that is necessary for RanGTP gradient-independent spindle assembly.

While we cannot entirely discount a contribution of centrosomes to gradient-free spindle assembly in the extract we favor the centromere-centric model for three reasons. First, the addition of purified centrosomes to Q/T

treated bead spindles did not induce spindle assembly, suggesting centrosomes alone are not sufficient (data not shown). Secondly, nuclei that lack clearly associated centrosomes go on to build spindles. Third, the Q/T sperm spindle assembly mechanism is absolutely dependent upon INCENP, which is a centromere-enriched protein and not a centrosome-associated factor. Indeed, recent work has shown that the centromere/kinetochore region of chromosomes provides a preferential site for microtubule assembly, and both CPC and the RanGTP system were implicated in this preference [25, 26]. While chromatin beads are sufficient to direct assembly of a bipolar array, they cannot entirely recapitulate chromatin-controlled microtubule assembly mechanisms since they lack the protein assemblies that normally concentrate at centromeres and kinetochores. Adaptation of the chromatin bead system by targeting the assembly of specific microtubule promoting activities to mimic particular “chromosomal” domains will be a valuable tool in the future.

Acknowledgements

We acknowledge all members of the Salmon and Mitchison labs as well as previous cell division group participants Chris Field, Sophie Dumont, Dan Needleman and Martin Wühr. We are also grateful to Rebecca Heald, Petr Kalab, and Karsten Weis for the FRET sensors as well as Alex Kelly and Hiro Funabiki for INCENP antibody. This work was supported by the American Cancer Society (grant PF0711401 to T.J. Maresca), the National Cancer Institute (grant CA078048-09 to T.J. Mitchison) and the National Institutes of Health (grant F32GM080049 to J.C. Gatlin and grant GM24364 to E.D. Salmon).

References

1. Kalab, P., Pralle, A., Isacoff, E.Y., Heald, R., and Weis, K. (2006). Analysis of a RanGTP-regulated gradient in mitotic somatic cells. *Nature* *440*, 697-701.
2. Kalab, P., Weis, K., and Heald, R. (2002). Visualization of a Ran-GTP gradient in interphase and mitotic *Xenopus* egg extracts. *Science (New York, N.Y)* *295*, 2452-2456.
3. Gruss, O.J., Carazo-Salas, R.E., Schatz, C.A., Guarguaglini, G., Kast, J., Wilm, M., Le Bot, N., Vernos, I., Karsenti, E., and Mattaj, I.W. (2001). Ran induces spindle assembly by reversing the inhibitory effect of importin alpha on TPX2 activity. *Cell* *104*, 83-93.
4. Nachury, M.V., Maresca, T.J., Salmon, W.C., Waterman-Storer, C.M., Heald, R., and Weis, K. (2001). Importin beta is a mitotic target of the small GTPase Ran in spindle assembly. *Cell* *104*, 95-106.
5. Wiese, C., Wilde, A., Moore, M.S., Adam, S.A., Merdes, A., and Zheng, Y. (2001). Role of importin-beta in coupling Ran to downstream targets in microtubule assembly. *Science (New York, N.Y)* *291*, 653-656.
6. Inoue, S., and Sato, H. (1967). Cell motility by labile association of molecules. The nature of mitotic spindle fibers and their role in chromosome movement. *The Journal of general physiology* *50*, Suppl:259-292.
7. Karsenti, E., Newport, J., Hubble, R., and Kirschner, M. (1984). Interconversion of metaphase and interphase microtubule arrays, as studied by the injection of centrosomes and nuclei into *Xenopus* eggs. *The Journal of cell biology* *98*, 1730-1745.
8. Karsenti, E., Newport, J., and Kirschner, M. (1984). Respective roles of centrosomes and chromatin in the conversion of microtubule arrays from interphase to metaphase. *The Journal of cell biology* *99*, 47s-54s.
9. Heald, R., Tournebize, R., Blank, T., Sandaltzopoulos, R., Becker, P., Hyman, A., and Karsenti, E. (1996). Self-organization of microtubules into bipolar spindles around artificial chromosomes in *Xenopus* egg extracts. *Nature* *382*, 420-425.
10. Colombie, N., Cullen, C.F., Brittle, A.L., Jang, J.K., Earnshaw, W.C., Carmena, M., McKim, K., and Ohkura, H. (2008). Dual roles of Incenp crucial to the assembly of the acentrosomal metaphase spindle in female meiosis. *Development (Cambridge, England)* *135*, 3239-3246.
11. Sampath, S.C., Ohi, R., Leismann, O., Salic, A., Pozniakovski, A., and Funabiki, H. (2004). The chromosomal passenger complex is required for chromatin-induced microtubule stabilization and spindle assembly. *Cell* *118*, 187-202.
12. Gadea, B.B., and Ruderman, J.V. (2006). Aurora B is required for mitotic chromatin-induced phosphorylation of Op18/Stathmin. *Proceedings of the National Academy of Sciences of the United States of America* *103*, 4493-4498.
13. Nemergut, M.E., Mizzen, C.A., Stukenberg, T., Allis, C.D., and Macara, I.G. (2001). Chromatin docking and exchange activity enhancement of RCC1 by histones H2A and H2B. *Science (New York, N.Y)* *292*, 1540-1543.
14. Cooke, C.A., Heck, M.M., and Earnshaw, W.C. (1987). The inner centromere protein (INCENP) antigens: movement from inner centromere to midbody during mitosis. *The Journal of cell biology* *105*, 2053-2067.

15. Mitchison, T.J., and Kirschner, M.W. (1985). Properties of the kinetochore in vitro. I. Microtubule nucleation and tubulin binding. *The Journal of cell biology* *101*, 755-765.
16. Oegema, K., Desai, A., Rybina, S., Kirkham, M., and Hyman, A.A. (2001). Functional analysis of kinetochore assembly in *Caenorhabditis elegans*. *The Journal of cell biology* *153*, 1209-1226.
17. Dasso, M., Seki, T., Azuma, Y., Ohba, T., and Nishimoto, T. (1994). A mutant form of the Ran/TC4 protein disrupts nuclear function in *Xenopus laevis* egg extracts by inhibiting the RCC1 protein, a regulator of chromosome condensation. *The EMBO journal* *13*, 5732-5744.
18. Klebe, C., Bischoff, F.R., Ponstingl, H., and Wittinghofer, A. (1995). Interaction of the nuclear GTP-binding protein Ran with its regulatory proteins RCC1 and RanGAP1. *Biochemistry* *34*, 639-647.
19. Carazo-Salas, R.E., Guarguaglini, G., Gruss, O.J., Segref, A., Karsenti, E., and Mattaj, I.W. (1999). Generation of GTP-bound Ran by RCC1 is required for chromatin-induced mitotic spindle formation. *Nature* *400*, 178-181.
20. Kalab, P., Pu, R.T., and Dasso, M. (1999). The ran GTPase regulates mitotic spindle assembly. *Curr Biol* *9*, 481-484.
21. Wilde, A., and Zheng, Y. (1999). Stimulation of microtubule aster formation and spindle assembly by the small GTPase Ran. *Science (New York, N.Y)* *284*, 1359-1362.
22. Tirnauer, J.S., Grego, S., Salmon, E.D., and Mitchison, T.J. (2002). EB1-microtubule interactions in *Xenopus* egg extracts: role of EB1 in microtubule stabilization and mechanisms of targeting to microtubules. *Molecular biology of the cell* *13*, 3614-3626.
23. Vader, G., Medema, R.H., and Lens, S.M. (2006). The chromosomal passenger complex: guiding Aurora-B through mitosis. *The Journal of cell biology* *173*, 833-837.
24. Kelly, A.E., Sampath, S.C., Maniar, T.A., Woo, E.M., Chait, B.T., and Funabiki, H. (2007). Chromosomal enrichment and activation of the aurora B pathway are coupled to spatially regulate spindle assembly. *Developmental cell* *12*, 31-43.
25. Torosantucci, L., De Luca, M., Guarguaglini, G., Lavia, P., and Degrossi, F. (2008). Localized RanGTP accumulation promotes microtubule nucleation at kinetochores in somatic mammalian cells. *Molecular biology of the cell* *19*, 1873-1882.
26. Tulu, U.S., Fagerstrom, C., Ferenz, N.P., and Wadsworth, P. (2006). Molecular requirements for kinetochore-associated microtubule formation in mammalian cells. *Curr Biol* *16*, 536-541.

Figure Legends

Figure 1. Bipolar spindles assemble around both DNA-coated beads and sperm nuclei although the kinetics of tubulin polymerization is faster around sperm nuclei. **(A)** Time-lapse fluorescence imaging of x-rhodamine tubulin during spindle assembly around DNA-coated beads (top row) and sperm nuclei with (bottom row) and without centrosomes (middle row). Note that the centrosome (arrow) becomes detached from the spindle structure during assembly. **(B)** Quantification of x-rhodamine tubulin fluorescence over time during bead (blue line) and sperm spindle (pink line) assembly. The bead spindle (from top row in 1A) reaches maximum fluorescence intensity ~30 minutes after microtubule polymerization begins. The sperm spindle (from middle row in 1A) achieves maximum fluorescence intensity within 10 minutes of the onset of microtubule polymerization. **(C)** Average tubulin fluorescence intensity of bead (N=8) and sperm (N=5) spindle assemblies over time. Samples were averaged after onset of tubulin polymerization because the lag phase for each spindle varied. Scale bars: 10 μm . Time in minutes:seconds.

Figure 2. Sperm nuclei, but not DNA-coated beads, support spindle assembly in the absence of a RanGTP gradient. **(A)** Representative micrographs of control, Ran T24N (T) and RanQ69L/RanT24N (Q/T) treated sperm and bead spindle assembly reactions. **(B)** Quantification of the structures assembled around sperm nuclei in control, Ran T24N and Q/T reactions. Control reactions had >90% bipolar spindles. Addition of T24N, which blocks RanGTP generation by RCC1 and therefore prevents SAF liberation from import receptors, severely compromised spindle assembly as only ~20% of structures were bipolar, while ~60% of nuclei had associated microtubule asters and ~20% had no associated microtubules. Nearly 80% of sperm nuclei formed bipolar spindles in the absence of a RanGTP gradient following Q/T treatment (N=3 independent experiments). Thus, global activation of SAFs in the absence of a chromatin localized RanGTP gradient still allows for localized microtubule polymerization and bipolar spindle assembly around sperm nuclei. **(C)** The YRC FRET probe exhibits reduced FRET efficiency (blue signal in the merged image) reflecting increased levels of GTP-bound Ran around chromatin in control reactions. Q/T treatment yields uniformly reduced FRET signal of the YRC probe revealing loss of a detectable RanGTP gradient even though spindles are assembled. **(D)** Addition of threefold molar excess of EB1 rescues sperm spindle assembly but not bead spindle assembly in the absence of a RanGTP gradient. **(E)** Quantification of the structures assembled around sperm nuclei in control, +T24N, +T24N+EB1 reactions. Control reactions had ~70% bipolar spindles while fewer than 10% of structures were bipolar following addition of T24N. The

percentage of bipoles was elevated to 50% following addition of a threefold molar excess of EB1 to T24N-treated reactions. The images show tubulin in red and beads in blue. For each graph, 100 structures were counted for each condition from at least 3 independent experiments. Scale bars: 10 μm .

Figure 3. INCENP is required for RanGTP gradient-independent spindle assembly. **(A)** Representative micrographs of mock depleted, INCENP depleted and gradient-free (Q/T) INCENP-depleted sperm and bead spindle assembly reactions. The merged images show tubulin in red and DNA in blue.

(B) Quantification of sperm nuclei structures in control, T and Q/T reactions in the presence and absence of INCENP (N=3 independent experiments). In mock-depleted extracts, ~90% of structures in control reactions are bipolar spindles, addition of T24N results in ~80% of structures having no associated microtubules and Q/T treatment yields mostly (~60%) bipolar spindles. INCENP depletion results in a range of microtubule structures around sperm nuclei including short bipolar spindles (~25%), asters (~40%) and naked DNA (~35%). 100% of sperm nuclei had no associated microtubules following the addition of T24N or Q/T to INCENP-depleted reactions. N=100 structures from at least 3 independent experiments for each condition. **(C)** INCENP levels are significantly reduced following immunodepletion with tubulin shown as a loading control. **(D)** Addition of an inhibitory MCAK antibody results in the formation of large microtubule arrays around sperm nuclei in both mock- and INCENP-depleted extracts. However, INCENP-depleted, RanGTP gradient-free (Q/T) extracts no longer assemble microtubule arrays in the vicinity of chromatin. Scale bars: 10 μ m.

Figure 4. Artificial enrichment of INCENP confers RanGTP gradient-free spindle assembly activity to DNA-coated beads. **(A)** Representative image of a bipolar spindle assembled around a hybrid bead cluster consisting of DNA beads and α -INCENP coated beads. In the merged images tubulin is in red, DNA-coated beads are in blue and all beads (DNA- and α -INCENP coated beads) are in green. **(B)** Representative micrographs of RanGTP gradient-free structures assembled around sperm nuclei (bipolar spindle), IgG hybrids (no microtubules) and α -INCENP hybrids, which support the assembly of both microtubule arrays and bipolar spindles. **(C)** Quantification of the total number of microtubule arrays and bipolar spindles observed around hybrids in 2 μ l samples of each condition (N= 2 independent experiments). \sim 4X as many microtubule arrays and $>$ 10X as many bipolar spindles were observed around α -INCENP hybrids relative to the control IgG hybrid clusters. **(D)** Comparable levels of the CPC components INCENP (upper panel) and Aurora B (middle and lower panels) are present on sperm and beads relative to the loading control the chromokinesin Xkid, which localizes throughout chromatin, as determined by western blot analysis. Both INCENP and Aurora B are highly enriched on the hybrid beads. Multiple higher molecular weight bands, one of which may be the IgG heavy chain, are evident in the shorter exposure of the Aurora B blot (lower panel) suggesting that Aurora B is hyper-phosphorylated on the anti-INCENP beads. Scale Bar: 10 μ m.

Supplemental Experimental Procedures

Extract preparation and spindle assembly reactions

CSF extracts were prepared from *Xenopus laevis* eggs and spindles were assembled as described previously [1-3] except the extract was filtered through a 0.8 μm syringe filter (Millipore) before use. Briefly, spindles were assembled from CSF extract containing either demembrated sperm nuclei (500/ μl) or 1-2 μl of DNA-coated beads cycled from interphase (with addition of 0.4mM CaCl_2) for 120 minutes before addition of CSF to drive the extract back into metaphase. Sperm spindles generally assembled within 45-60 minutes. After 45 minutes, chromatin-beads were isolated from the extract and re-suspended in fresh CSF extract. Tubulin was visualized with addition of purified bovine tubulin (20 $\mu\text{g}/\text{ml}$) directly labeled with X-rhodamine (Invitrogen) as described previously [4, 5]. All experiments were repeated 2-3 times using different extract preparations.

Q/T reactions

RanQ69L, RanT24N were bacterially expressed and purified as previously described [6]. To form spindles in the absence of a RanGTP gradient, interphase sperm nuclei were assembled and incubated for at least two hours in interphase, which we believe promoted more robust kinetochore assembly, before adding back CSF extract. After ~15 minutes, to allow for the onset of nuclear envelope breakdown, ~10-15 μM RanQ69L and 30 μM RanT4N were simultaneously added to the extract. Despite the fact that ~8 μM RanT24N was sufficient to block both bead and sperm spindle assembly, we added excess RanT24N (30

μM) to ensure no SAFs could be activated. Furthermore, RanQ69L requirements varied between extracts and RanQ69L preparations. Depending on the extract and the protein preparation as low as $\sim 2 \mu\text{M}$ RanQ69L could begin yielding spindles in the presence of T24N. For all the experiments presented here we added $\sim 10 \mu\text{M}$ RanQ69L. No concentration of RanQ69L yielded bead spindles in the presence of RanT24N. Gradient-free spindles generally formed after ~ 45 -60 minutes.

Time-lapse fluorescence microscopy

Sperm and bead spindle assembly were imaged on an inverted Nikon Eclipse TE2000-U microscope stand equipped with a cooled CCD Orca ER camera (Hamamatsu) using a Nikon 40X/1.3 NA plan-Fluor differential interference contrast (DIC) objective. Five-seven μl of an assembly reaction was squashed under a 22X22 mm coverslip and sealed with valap. For sperm spindle assembly, imaging was started immediately after the addition of fresh CSF extract while chromatin beads could be isolated, re-suspended in fresh extract and stored on ice for several hours before preparing a live squash that would assemble spindles. 500 ms exposures were acquired every 1 minute. All extract was filtered as described above and the room was kept at ~ 18 - 20°C during imaging.

Quantification of Fluorescence Intensity

X-rhodamine-labeled tubulin intensity was quantified for each frame of a timelapse of spindle assembly using MetaMorph (Molecular Devices) software.

In brief, a larger and smaller circular region was drawn manually, using the ellipse region tool, around the assembling spindle and moved accordingly for each frame so that the two regions always contained the structure. The area and integrated intensity of both regions for every frame were then exported from the “region measurements” window in Metamorph to an Excel (Microsoft) spreadsheet for calculating the background signal and the total fluorescence intensity. The following equations were applied: Background signal = $(\text{Integrated fluorescence intensity}_{\text{big area}} - \text{Integrated fluorescence intensity}_{\text{small area}}) / (\text{Area}_{\text{big}} - \text{Area}_{\text{small}})$. Total intensity = $\text{Integrated fluorescence intensity}_{\text{small area}} \times (\text{Background signal} \times \text{Small Area})$. The total intensity for each frame of the time-lapse movie is reported in the graphs.

FRET analysis

YRC and YIC were bacterially expressed and purified as previously described [7]. To assay for gradients, 1.2 μM of the YRC FRET probe or 1.8 μM of the YIC FRET probe were added to reactions containing assembled spindles and incubated for 10-15 minutes before visualization. Squashes were prepared as described and 200 ms exposures for the Cy3 (tubulin), CFP, YFP and FRET channels were acquired using a Nikon 40X/1.3 NA plan-Fluor differential interference contrast (DIC) objective on an inverted Nikon Eclipse Ti stand equipped with an iXON EMCCD camera (Andor Technology). For YFP imaging an ET500/20X excitation filter and ET535/30M emission filter was used. For CFP imaging an ET430/24X exciter and ET470/24M emitter was used. An ET

CFP/YFP dichroic mirror was used for imaging both YFP and CFP. The filters and dichroic mirror were made by Chroma Technology. FRET/CFP ratio image was acquired utilizing the Metamorph (Molecular Devices) ratio images function where the FRET image was set to the numerator and CFP to the denominator and the ratio range was set from 1-3 for the YRC probe and 1.75-2.5 for the YIC probe. The resulting ratio image was pseudocolored in Metamorph.

INCENP depletion and MCAK inhibition

INCENP-depletion was carried out as previously described [8]. Briefly, 8 μg of affinity purified anti-INCENP or control IgG was coupled to protein-A Dynabeads (Invitrogen) and 50 μl of extract was subjected to two one hour rounds of incubation. α -MCAK arrays were assembled by the addition of ~ 0.05 mg/ml inhibitory MCAK antibody [9] to pre-formed structures and incubating for 15 minutes.

INCENP hybrids

For INCENP hybrids, the beads from both rounds of immunodepletion were pooled and washed twice with 200 μl XB buffer (10 mM Hepes pH7.7, 1 mM MgCl_2 , 0.1 mM CaCl_2 , 100 mM KCl, 50 mM Sucrose) before being resuspended in 20 μl XB. 0.2 μl of either α -INCENP- or α -IgG bound Protein-A beads (Dyna; Invitrogen) were then mixed with 3 μl of DNA beads, diluted into 20 μl of extract and released into interphase by the addition of 0.4mM CaCl_2 . After 90 minutes, 20 μl of CSF extract was added to each reaction and incubated for an additional

45 minutes. The beads were retrieved and re-suspended in 100 μ l of fresh CSF extract and incubated for 60 minutes to assemble hybrid bead structures.

Isolation of Chromatin-associated Proteins from Sperm Chromosomes and DNA Beads

Chromatin-associated proteins were isolated from sperm chromosomes and chromatin beads as previously described [10, 11] with the following changes. Metaphase chromosomes were pelleted through a 60% sucrose cushion in Bead buffer 1 plus 0.05% Triton X-100 [10]. The chromosomal pellet was then resuspended in 1X Laemmli buffer.

Supplemental Figure

Figure S1. Quantification of bipolar sperm spindle assembly for titrations of RanQ69L and RanT24N. Addition of concentrations greater than 8 μ M RanT24N to extract completely blocked the assembly of either bead spindles or sperm spindles. For this preparation of RanQ69L, bipolar spindles began to assemble in the presence of 8 μ M RanT24N at concentrations of RanQ69L higher than ~5 μ M.

Figure S2. Q/T treatment flattens the SAF gradient around chromatin. FRET efficiency of the YIC probe is increased around chromatin (red signal in merged image) indicating localized SAF release from importins (upper panels).

However, the SAF gradient is no longer detectable following Q/T treatment (lower panels).

Supplemental Movies

Movie 1: Time-lapse fluorescence imaging of bead spindle assembly.

Movie 2: Time-lapse fluorescence imaging of sperm spindle assembly in the absence of centrosomes.

Movie 3: Time-lapse fluorescence imaging of sperm spindle assembly in the presence of centrosomes.

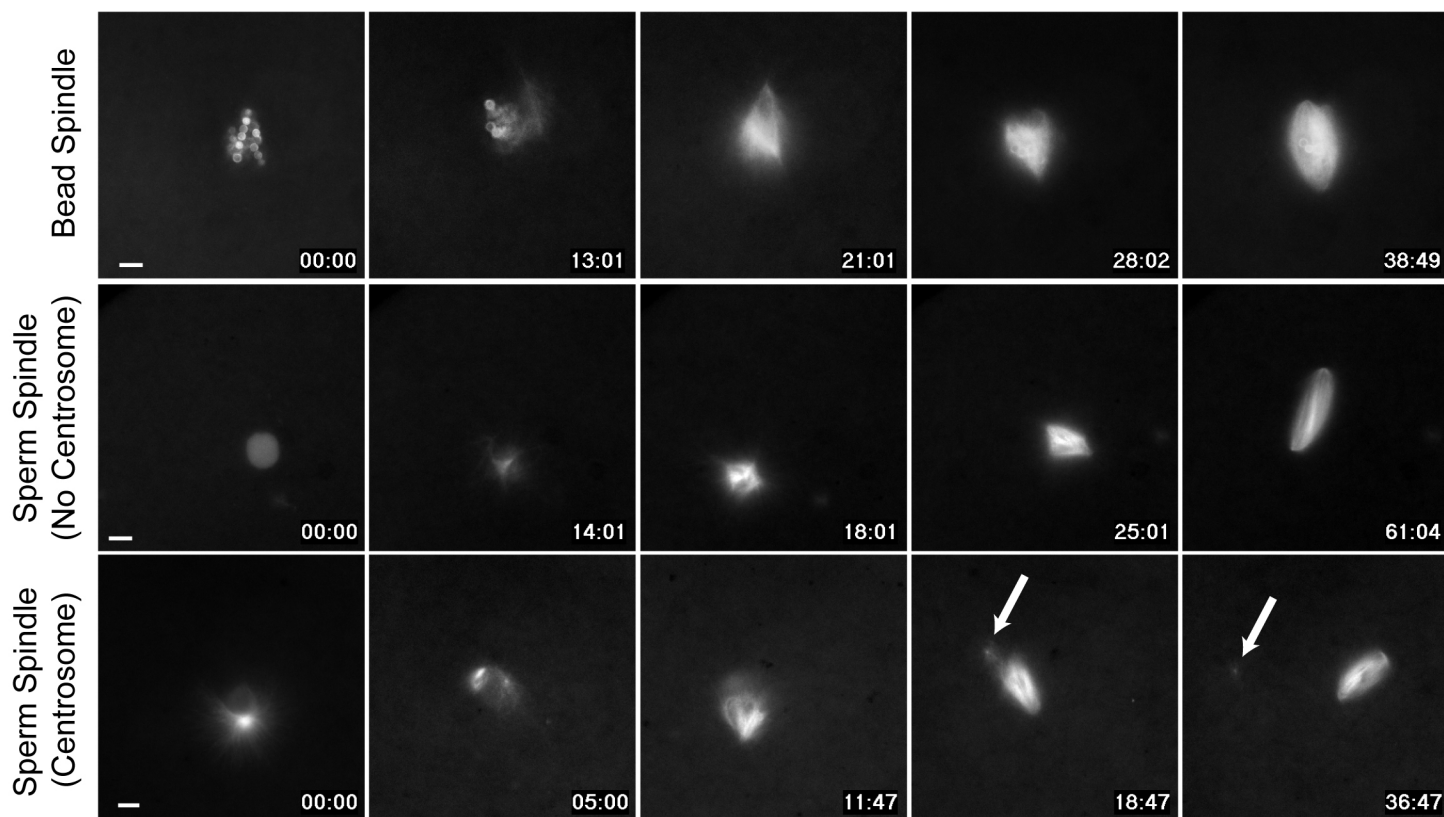
Supplemental References

1. Desai, A., Murray, A., Mitchison, T.J., and Walczak, C.E. (1999). The use of *Xenopus* egg extracts to study mitotic spindle assembly and function in vitro. *Methods in cell biology* *61*, 385-412.
2. Hannak, E., and Heald, R. (2006). Investigating mitotic spindle assembly and function in vitro using *Xenopus laevis* egg extracts. *Nature protocols* *1*, 2305-2314.
3. Murray, A.W. (1991). Cell cycle extracts. *Methods in cell biology* *36*, 581-605.
4. Hyman, A., Drechsel, D., Kellogg, D., Salser, S., Sawin, K., Steffen, P., Wordeman, L., and Mitchison, T. (1991). Preparation of modified tubulins. *Methods in enzymology* *196*, 478-485.
5. Sawin, K.E., and Mitchison, T.J. (1991). Poleward microtubule flux mitotic spindles assembled in vitro. *The Journal of cell biology* *112*, 941-954.
6. Bischoff, F.R., Klebe, C., Kretschmer, J., Wittinghofer, A., and Ponstingl, H. (1994). RanGAP1 induces GTPase activity of nuclear Ras-related Ran. *Proceedings of the National Academy of Sciences of the United States of America* *91*, 2587-2591.
7. Kalab, P., Weis, K., and Heald, R. (2002). Visualization of a Ran-GTP gradient in interphase and mitotic *Xenopus* egg extracts. *Science (New York, N.Y)* *295*, 2452-2456.

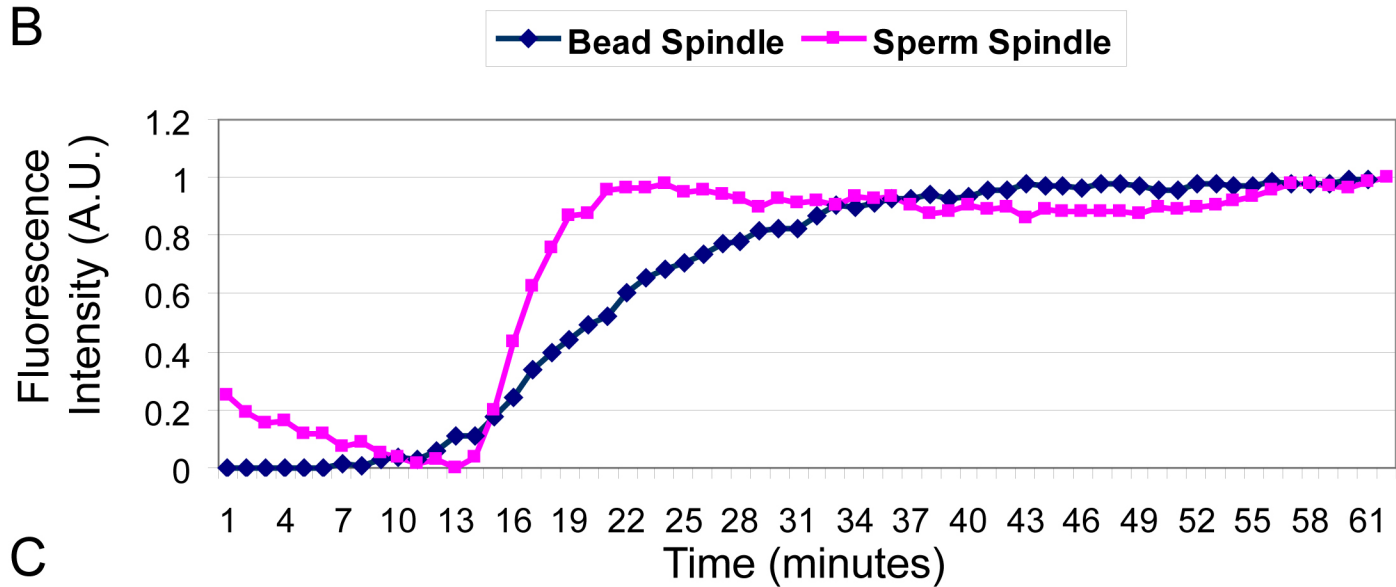
8. Sampath, S.C., Ohi, R., Leismann, O., Salic, A., Pozniakovski, A., and Funabiki, H. (2004). The chromosomal passenger complex is required for chromatin-induced microtubule stabilization and spindle assembly. *Cell* *118*, 187-202.
9. Mitchison, T.J., Maddox, P., Gaetz, J., Groen, A., Shirasu, M., Desai, A., Salmon, E.D., and Kapoor, T.M. (2005). Roles of polymerization dynamics, opposed motors, and a tensile element in governing the length of *Xenopus* extract meiotic spindles. *Molecular biology of the cell* *16*, 3064-3076.
10. Budde, P.P., Kumagai, A., Dunphy, W.G., and Heald, R. (2001). Regulation of Op18 during spindle assembly in *Xenopus* egg extracts. *The Journal of cell biology* *153*, 149-158.
11. Funabiki, H., and Murray, A.W. (2000). The *Xenopus* chromokinesin Xkid is essential for metaphase chromosome alignment and must be degraded to allow anaphase chromosome movement. *Cell* *102*, 411-424.

Figure 1

A



B



C

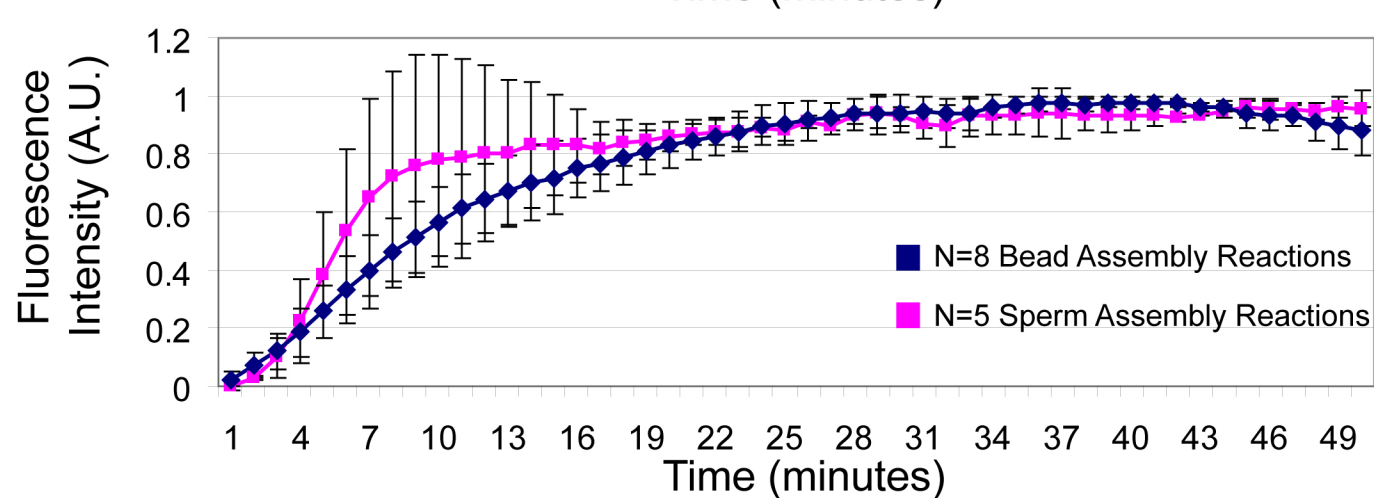


Figure 2

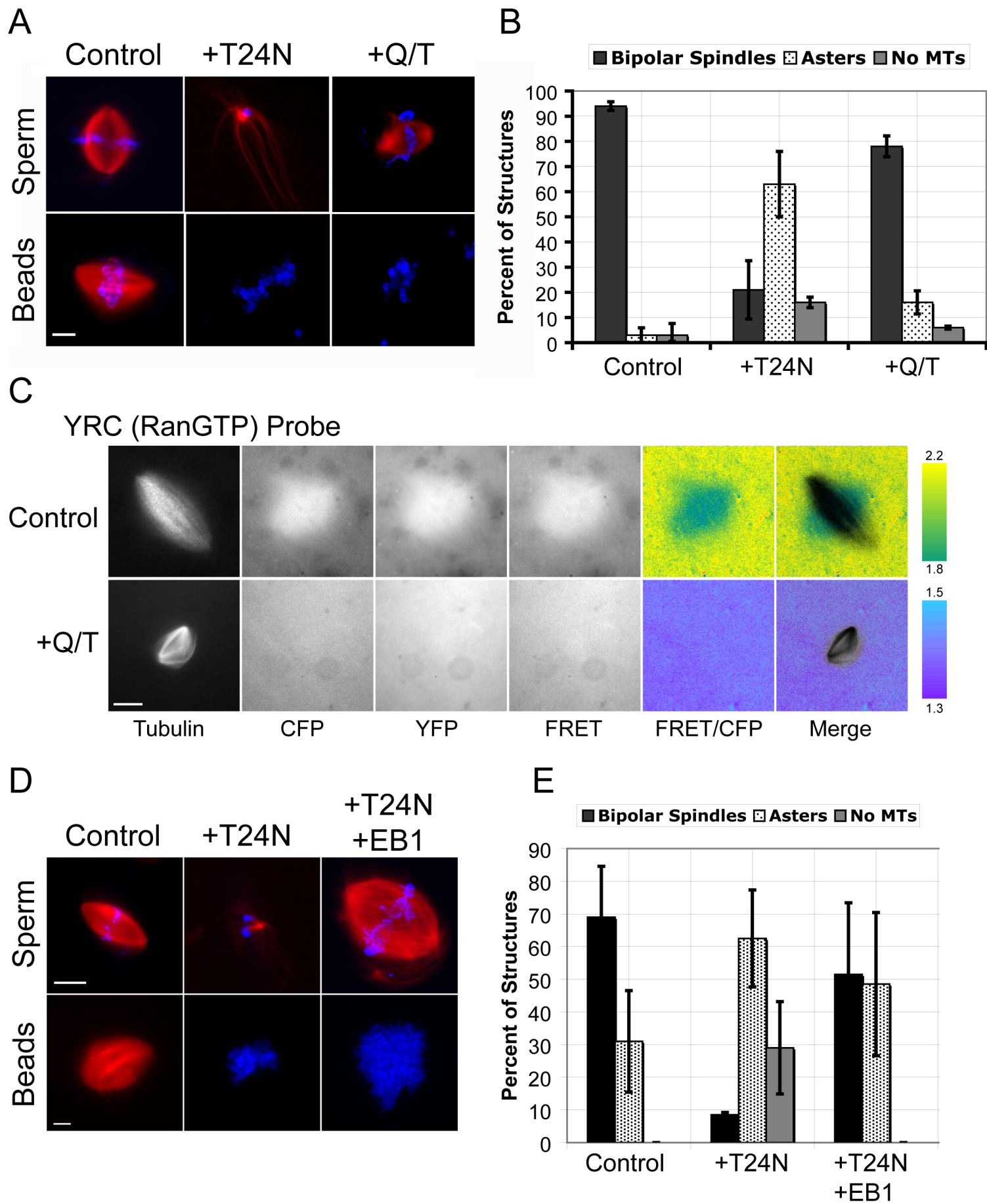
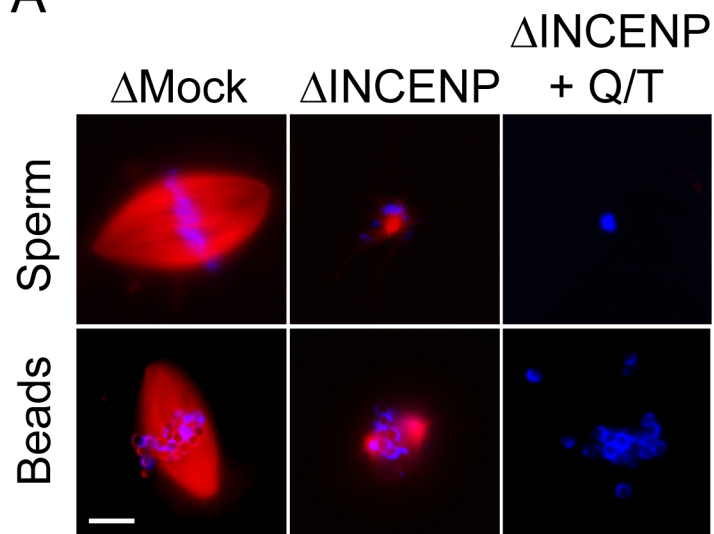
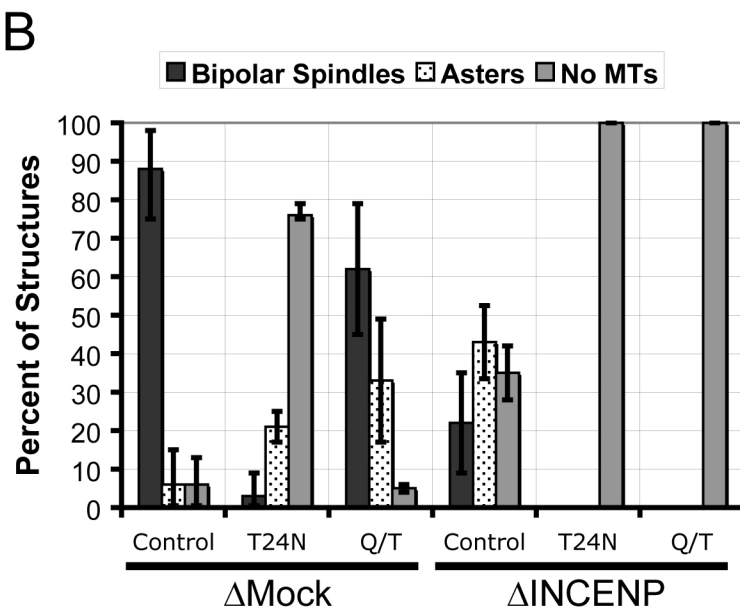


Figure 3

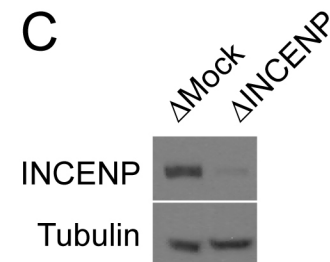
A



B



C



D

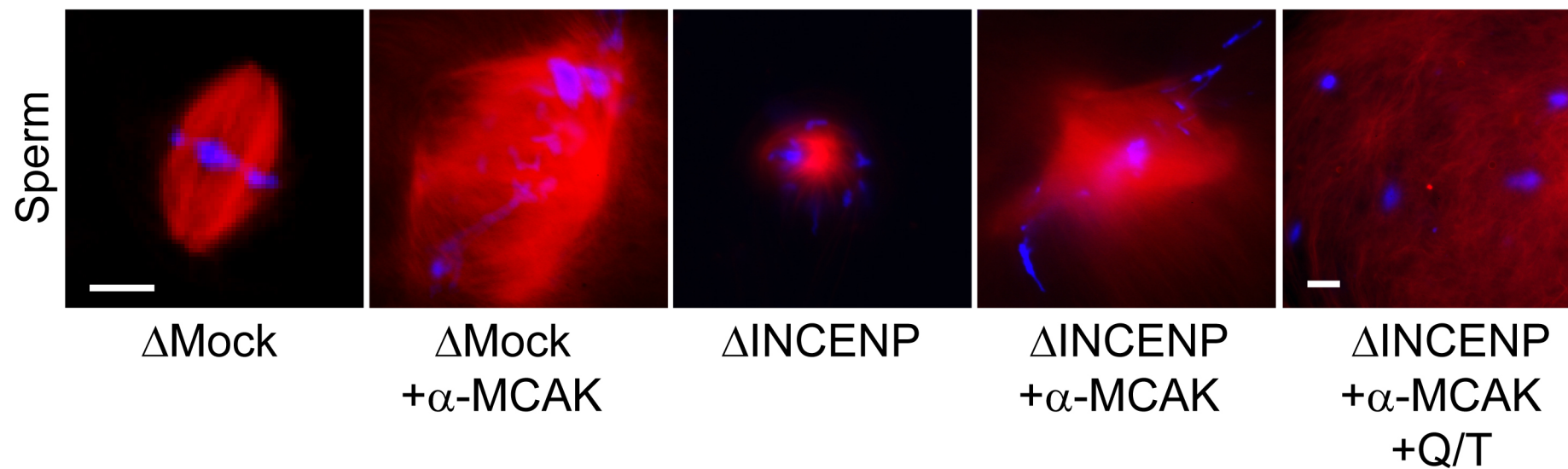
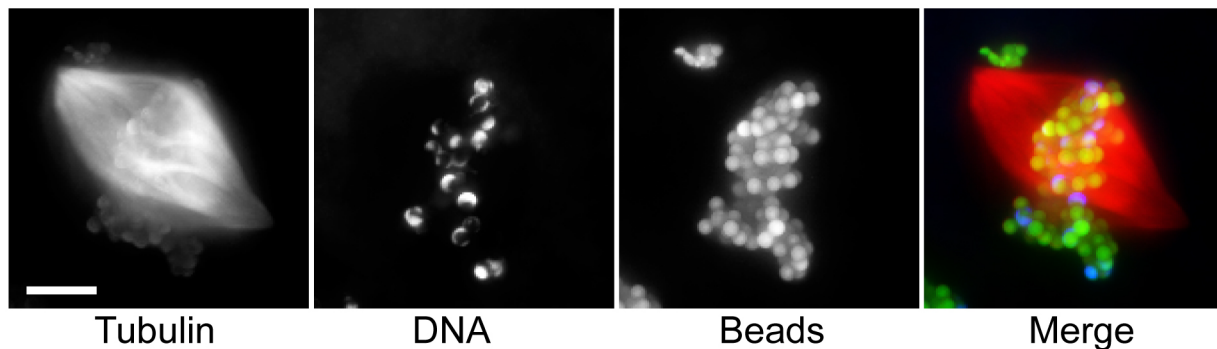
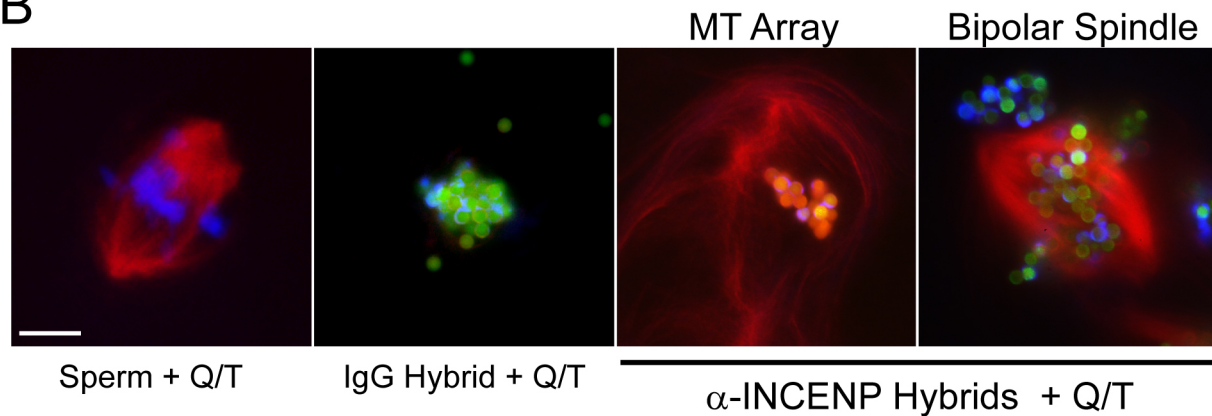


Figure 4

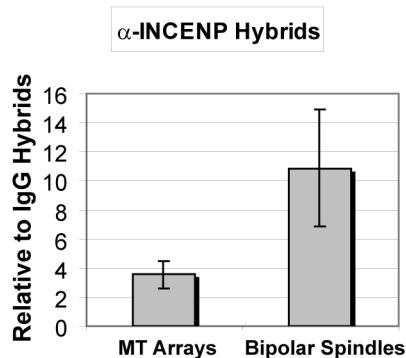
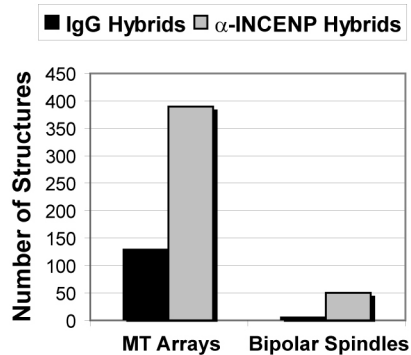
A



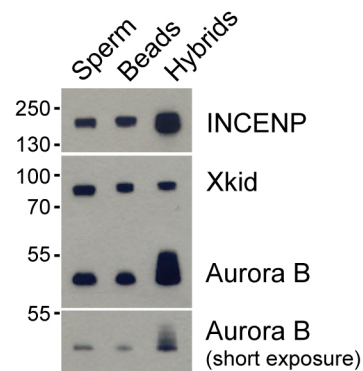
B



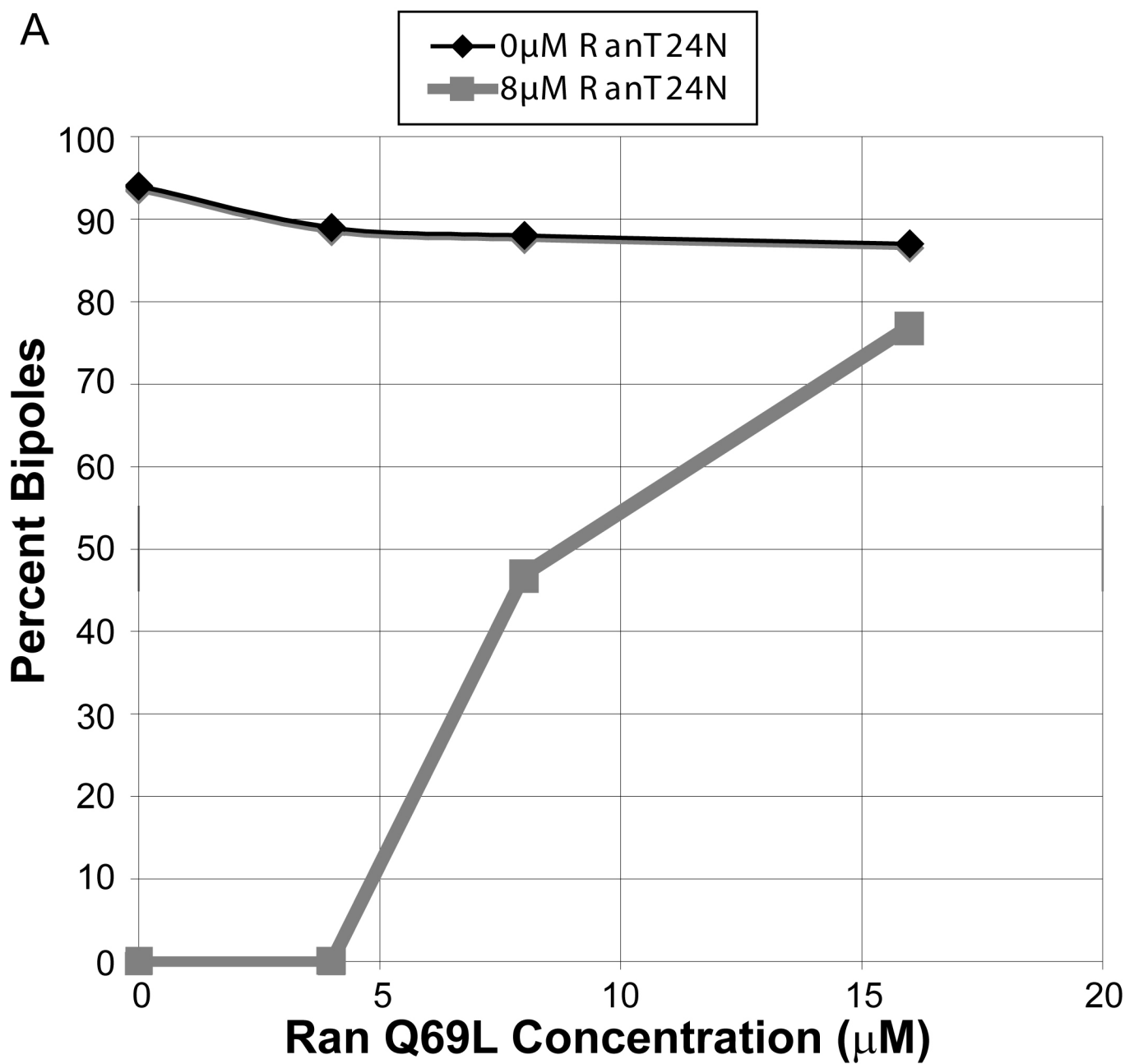
C



D



Supplemental Figure 1



Supplemental Figure 2

YIC (SAF) Probe

